Influence of Material Characteristics on the Abrasive Wear Response of Some Hardfacing Alloys

A.K. Jha, B.K. Prasad, R. Dasgupta, and O.P. Modi

(Submitted 2 May 1998; in revised form 17 November 1998)

This study examines the abrasive wear behavior of two iron-base hardfacing materials with different combinations of carbon and chromium after deposition on a steel substrate. Effects of applied load and sliding distance on the wear behavior of the specimens were studied. Operating material removal mechanisms also were analyzed through the scanning electron microscopy (SEM) examination of typical wear surfaces, subsurface regions, and debris particles.

The results suggest a significant improvement in the wear resistance of the hardfaced layers over that of the substrate. Further, the specimens overlaid with the material with low carbon and high chromium contents attained better wear resistance than the one consisting of more carbon but less chromium. The former specimens also attained superior hardness.

Smoother abrasion grooves on the wear surfaces and finer debris formation during the abrasion of the hardfaced samples were consistent with wear resistance superior to that of the substrate.

Keywords hardfacing alloys, material removal mechanisms, microstructure-hardness-abrasion property correlation, surface engineering, wear

1. Introduction

Wear related failure of machinery components counts as one of the major reasons for inefficient working of machines in a variety of engineering applications (Ref 1, 2). Many such applications involve handling of abrasive materials or contact with the material in service. Abrasion is one of the important and commonly observed wear modes in these cases (Ref 1-4).

Abrasive wear behavior of steels has been studied in earlier investigations (Ref 2-6). Fundamental aspects of the mode of wear (including operative wear mechanisms, the nature of the debris particles formed, and the kind of surface and subsurface damage under a given set of experimental conditions) have been evaluated (Ref 2-6). Other aspects studied include the extent and mode of damage caused to the abrasive particles during wear. Further, the relevance of the bench tests with bonded abrasives to the wear in agricultural machinery has been discussed by Richardson (Ref 5).

Wear resistance of materials can be improved through bulk treatment and surface modification (Ref 6, 7). While bulk treatment has been practiced for a long time, surface treatment is fairly recent and gaining importance (Ref 7). Because wear is a surface phenomenon, it is possible to use a relatively inferior bulk material for a specific (wear related) application by modifying the surface characteristics of the material economically.

A variety of techniques/materials exist for modifying the surface properties of substrates. However, their success depends on an appropriate selection of the techniques/materials depending on the application of the modified components. This emphasizes the need to characterize the modified surfaces accordingly. Among many proven techniques of surface modification, hardfacing has been especially effective in cases not requiring close dimensional tolerances. It has been reported that iron-base alloys containing different combinations of chromium and carbon are widely used (Ref 8) for depositing on different steel substrates by the technique of hardfacing. Thus, the material composition of the deposited mass influences the wear resistance of the layers. Interestingly, in spite of several recommended applications (of which abrasive wear situations form a major share) for hardfacing materials (Ref 9), very limited scientific information is available pertaining to behavior of materials under different experimental conditions (Ref 7).

An attempt has been made in this study to understand the influence of different hardfacings on the high stress abrasion resistance of a steel, to assess the effects of applied load and sliding distance on the wear behavior of the specimens, and to analyze the operating wear mechanisms.

A.K. Jha, B.K. Prasad, R. Dasgupta, and **O.P. Modi,** Regional Research Laboratory (CSIR), Near Habibganj Naka, Bhopal 462 026, India.

2. Experimental Procedures

2.1 Specimen Preparation

Two types of hardfacing materials were selected. Table 1 represents the chemical compositions of both the hardfacing alloys and the substrate materials. A 3 mm thick layer was deposited using the hardfacing materials (Table 1) on a 6 mm thick steel substrate by manual arc welding technique. Specimens for metallographic and wear studies were cut from the overlaid plates using a diamond cutting wheel.

2.2 Wear Tests

Abrasive wear tests were conducted using a two-body abrasion tester (Suga Test Instruments Company Ltd., Tokyo, Ja-

pan). Metallographically polished flat rectangular test pieces (of size 40 mm × 35 mm × 4 mm) were made to move in reciprocating motion under load against the abrasive medium. The abrasive medium in this case was 180 μm silicon carbide particles bonded on an emery paper rigidly held on a metallic wheel. The test procedure was adopted from Prasad et al. (Ref 10) wherein fresh abrasive has been used in each case. A schematic view of the test apparatus is given in Fig. 1. Tests were conducted over a range of applied loads (3-7 N) and sliding distances (25-160 m). Wear rates were computed by a weight loss technique.

2.3 Metallographic Studies

Transverse sections of the hardfaced specimens were placed in polymeric mounts after wear tests and were polished by using standard metallographic practices for microstructural examination. Specimens were etched with 1% nital. Optical as well as scanning electron microscopy (SEM) was used for microstructural characterization of the samples. Worn surfaces and debris particles were also examined using SEM. The iron debris was separated from the used abrasive with a magnet and mounted on a brass stud using double-sided tape. The specimens were sputtered with gold prior to SEM examination.

3. Results

3.1 Microstructure and Hardness

Figure 2 shows the microstructural features of the hardfaced specimens. Good bonding between the hardfaced layer, L, and the substrate, S, are shown in Fig. 2(a). The substrate comprised ferrite (labeled A) plus pearlite (labeled B) in Fig. 2(b). The microconstituents of the hardfaced layer alloy 1 (Table 1) were primary chromium containing carbides in the dendrites (region labeled C) and austenite plus carbides in the interden-

Table 1 Chemical composition and hardness of the hardfacing alloys and substrate material

Material	Composition, wt%					Vickers Hardness
	C	Mn	Si	Cr	Fe	
Hardfacing alloy 1	0.5	0.3	0.45	6.5	bal	650
Hardfacing alloy 2	2.5	1.5	0.60	2.7	bal	550
Substrate	0.18	0.40	0.1	…	bal	150

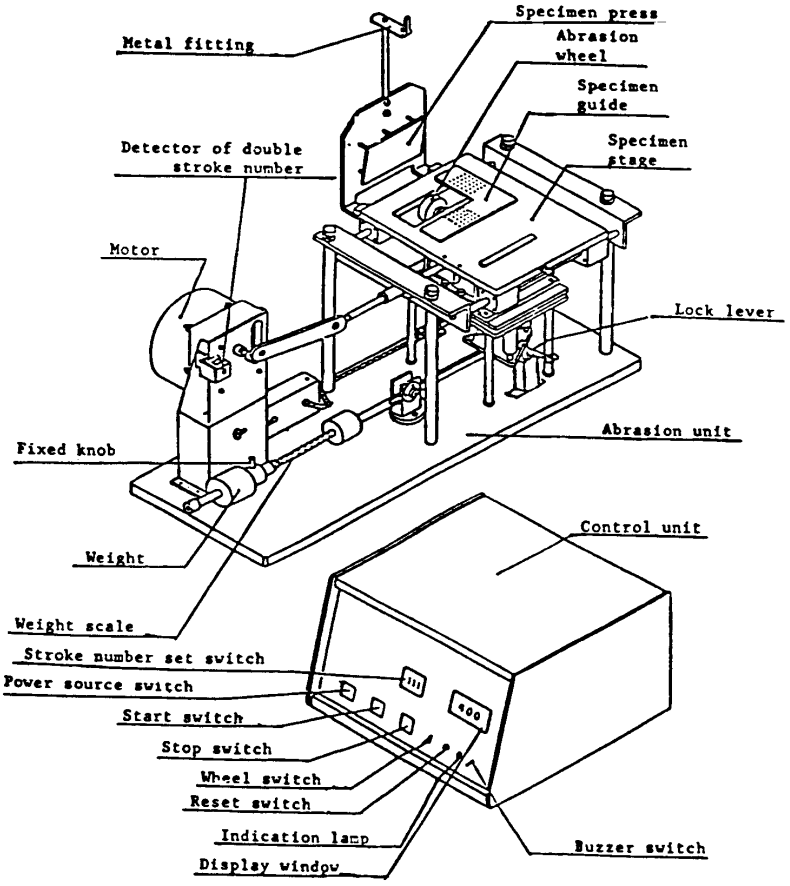

Fig. 1 Schematic of the abrasion tester

dritic region (labeled D) in Fig. 2(c). Similarly, the hardfaced layer alloy 2 (Table 1) showed the presence of dendrites of primary austenite (in the region labeled E in Fig. 2d) surrounded by the eutectic austenite plus carbide in the interdendritic region (labeled F in Fig. 2d). Microstructural characterization of the specimens has been reported by Dasgupta et al. (Ref 11).

Hardness of the specimens is shown in Table 1. The hardfaced layer of alloy 1 exhibited maximum hardness. This was followed by that of the hardfaced layer of alloy 2, while the substrate showed minimum hardness.

3.2 Wear Response

Wear rate of the specimens is plotted as a function of sliding distance at different loads in Fig. 3. The wear rate was observed to be marginally affected by the distance traversed except in the case of the substrate at 7 N. However, within that, a reduction in wear rate with distance was noted at the applied load of 3 N while a reversal in the trend was observed at 7 N (Fig. 3). The wear response of the substrate at 7 N was somewhat different in that the wear rate initially increased with distance while it reduced at a longer distance. Further, wear rate in general increased with load (Fig. 3).

Figure 4 represents the wear behavior of the specimens after traversing a typical distance of 78 m at different loads. The results indicate a significant improvement in wear resistance (inverse of wear rate) of the hardfaced layers over that of the substrate. The improvement was more pronounced at higher loads. Moreover, the hardfaced layer of alloy 1 attained maximum wear resistance (Fig. 4).

3.3 Wear Surfaces

Wear surfaces of the specimens are shown in Fig. 5. Long continuous grooves with damaged regions were observed in all the cases. The depth of the abrasion grooves and surface damage was maximum for the substrate (Fig. 5a). More fine grooves with reduced depth and less damaged regions were features of the wear surfaces of the hardfaced layers (Fig. 5b, c). The extent of damage increased in the case of the hardfaced layer of alloy 2 (Fig. 5c) compared to the layer of alloy 1 (Fig. 5b).

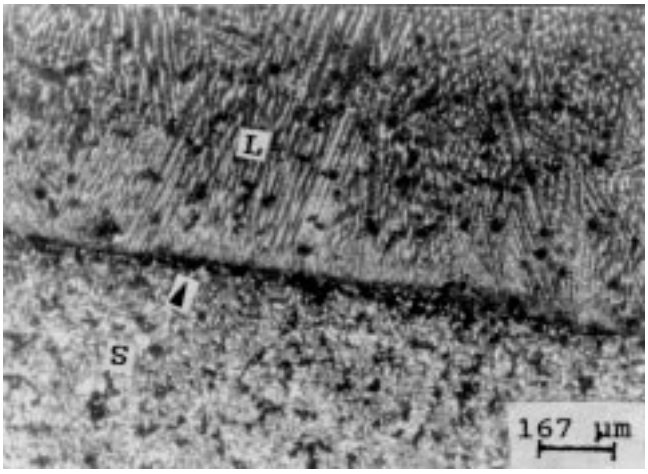

(a)

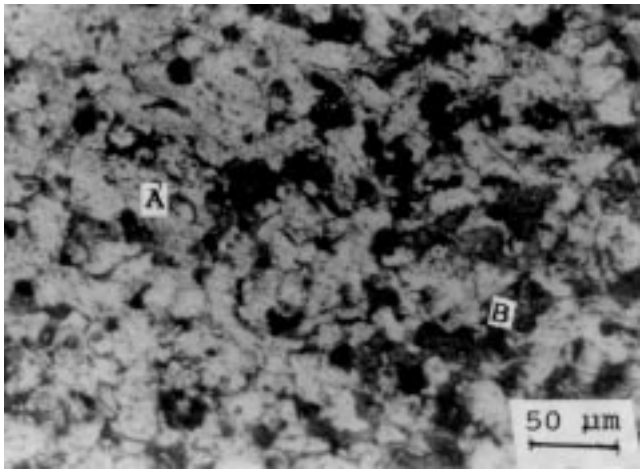

(b)

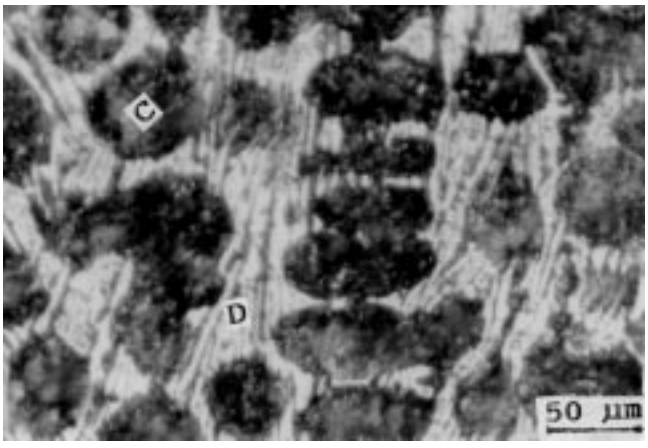

(c)

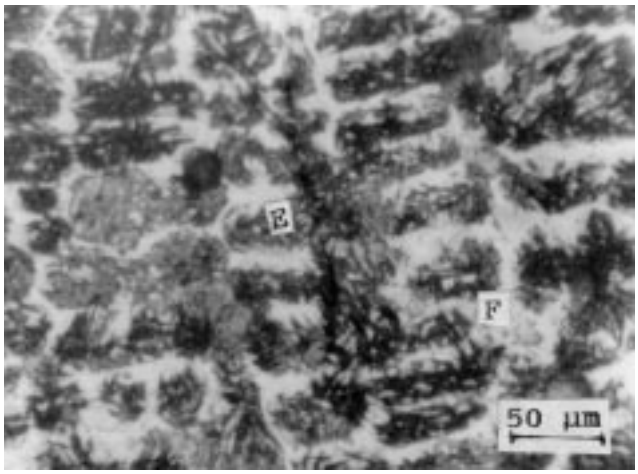

(d)

Fig. 2 Microstructure of (a) the specimen hardfaced with alloy 1, (b) a magnified view of the substrate, (c) a magnified view of the hardfacing layer of alloy 1, and (d) hardfacing layer of alloy 2. L, hardfaced layer; S, substrate; A, ferrite; B, pearlite; C, primary chromium carbide; D, austenite plus carbide; E, primary austenite; F, eutectic austenite plus carbide

3.4 Debris

Figure 6 shows the micrographs of the debris particles collected after a sliding distance of 78 m at a load of 7 N. Long machining chips (Fig. 6a, region marked A) and large flakes (Fig. 6b, region marked B) were observed in the case of the substrate. The debris in the case of the hardfaced layers was similar in nature but was much finer (Fig. 6c, regions marked A and B) than that of the substrate (Fig. 6a, b).

3.5 Subsurface Regions

The subsurface regions of the samples after abrasion tests at a sliding distance of 78 m and a load of 7 N are shown in Fig. 7. The substrate revealed the presence of large bulky masses (Fig. 7a, region marked A) that were in a process of being separated from the bulk (Fig. 7a, region marked B). Practically identical microstructural features of regions A and B are also shown in Fig. 7(a). On the contrary, relatively smaller masses were attached to the bulk in the case of the hardfaced layers (Fig. 7b, c) than the substrate (Fig. 7a). Presence of microcracks was observed in subsurface regions of the hardfaced layer 2 (Fig. 7c).

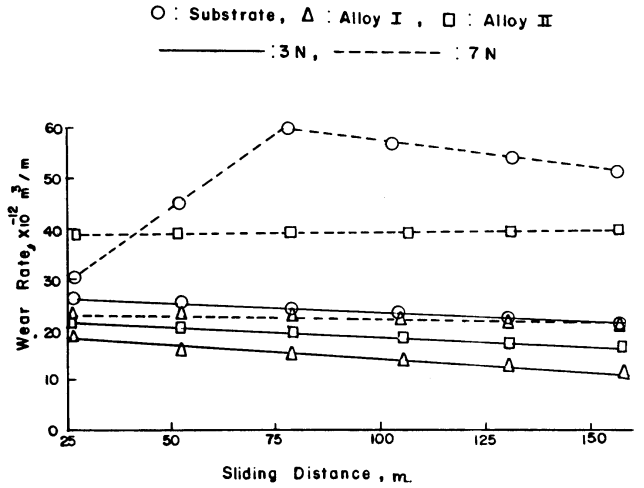

Fig. 3 Wear rate of the substrate and hardfacing alloys as a function of sliding distance at different loads

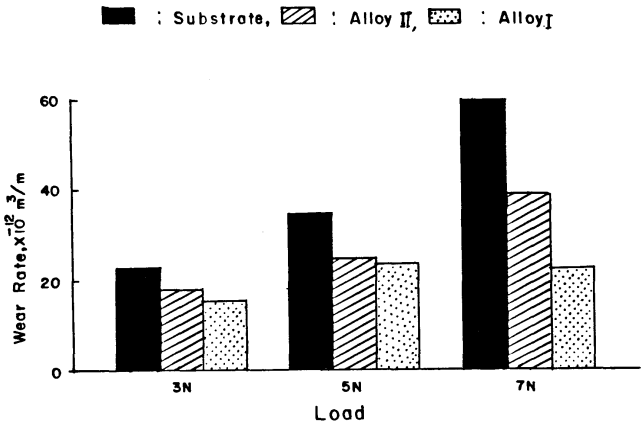

Fig. 4 Wear rate of the substrate and hardfacing alloys after a typical sliding distance of 78 m at different loads

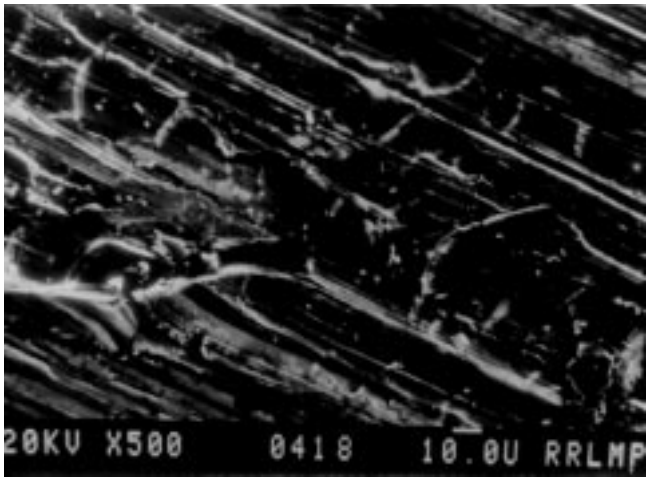

(a)

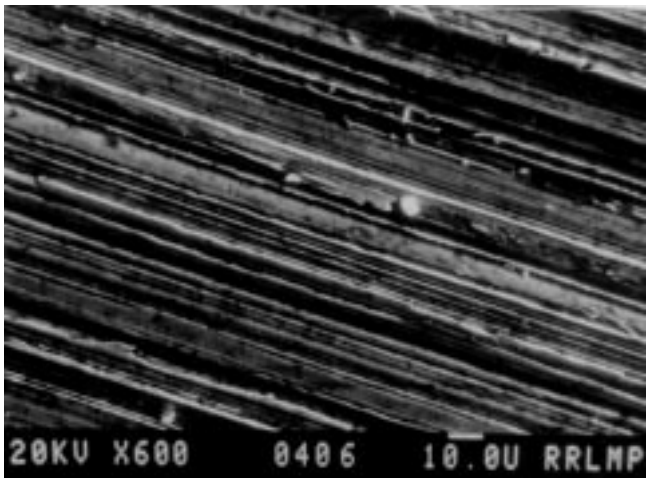

(b)

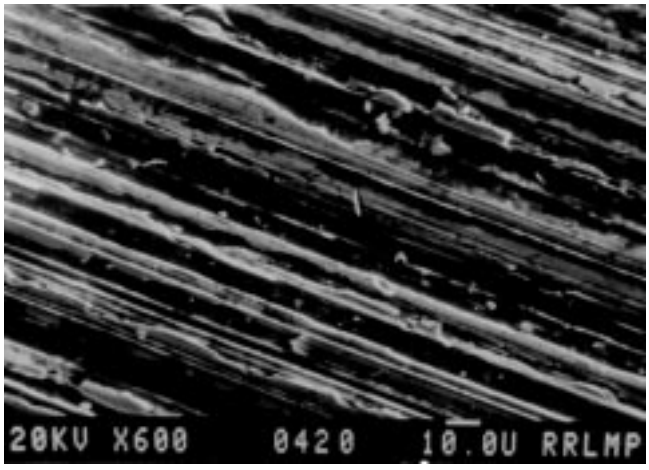

(c)

Fig. 5 Worn surfaces of (a) the substrate, (b) the hardfacing alloy 1, and (c) the hardfacing alloy 2 indicating continuous grooves and damaged regions after a sliding distance of 78 m at a load of 7 N

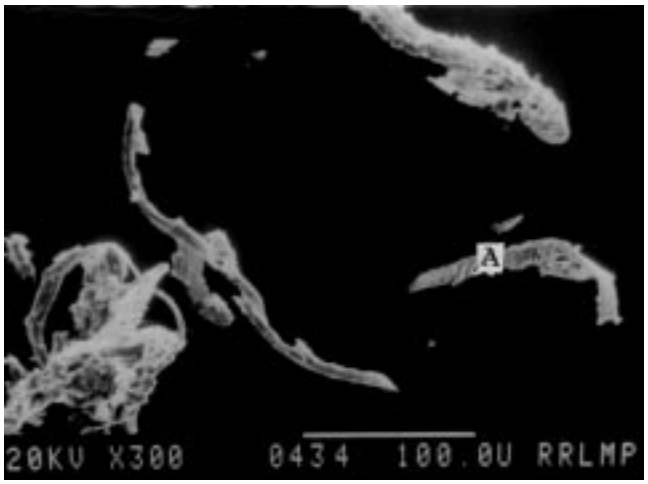

(a)

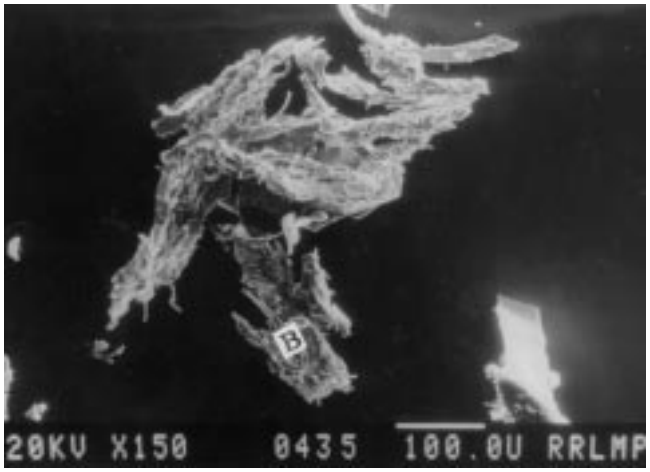

(b)

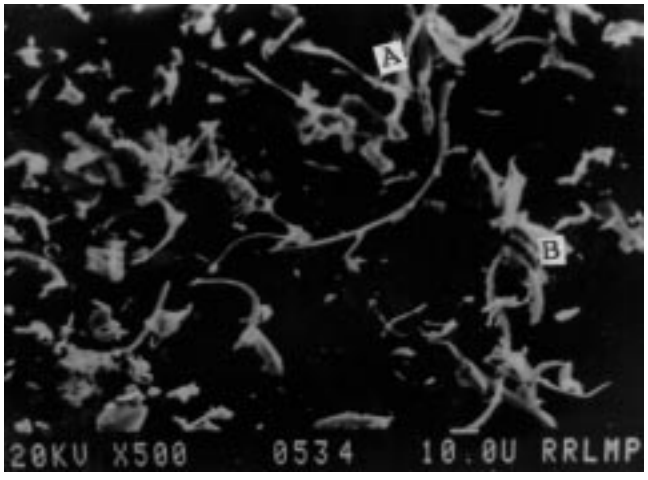

(c)

Fig. 6 Micrographs of (a) and (b) the debris of the substrate and (c) hardfacing alloy 1 after a sliding distance of 78 m at a load of 7 N. A, machining chip; B, deformed flake

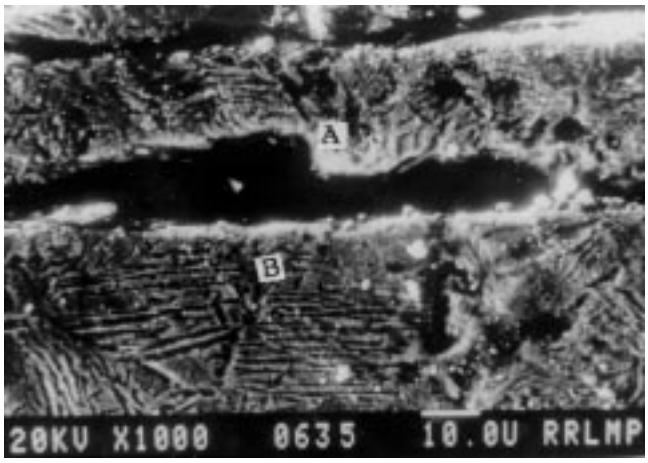

(a)

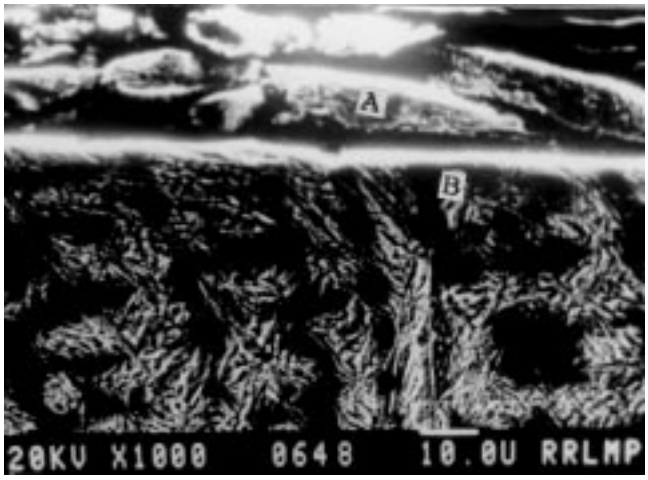

(b)

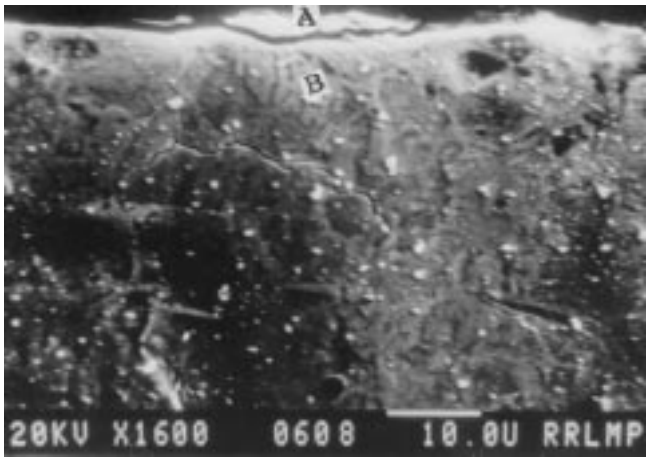

(c)

Fig. 7 Micrographs of the transverse sections of the worn surfaces of (a) the substrate, (b) the hardfacing alloy 1, and (c) the hardfacing alloy 2, after a sliding distance of 78 m at a load of 7 N. A, region in a process of being separated from the bulk; B, bulk

4. Discussion

Hardness values of the specimens agreed with their microstructural features. The existence of complex carbide (chromium containing) particles in a considerable quantity (Fig. 2c, d) imparted significantly high hardness values to the hardfaced layers. The hardness value of the substrate (i.e. the steel) was low as it comprised ferrite plus pearlite (Fig. 2b). The high chromium content of the hardfaced layer 1 formed chromium containing carbide in large quantity (Fig. 2c). On the contrary, in the hardfaced layer 2 (Table 1), less chromium (although it contained more carbon) led to the formation of reduced quantity of chromium carbide and more of austenite (Fig. 2d). Accordingly, the hardfaced layer of alloy 1 attained more hardness than the hardfaced layer of alloy 2 (Table 1).

The wear response of the samples improved with hardness (Fig. 2). Accordingly, the hardfaced layer (alloy 1) comprising maximum hardness (Table 1) exhibited the least wear rates (Fig. 3, 4). This was followed by the wear rates of the hardfaced layer of alloy 2 and those of the substrate in order of decreasing hardness. Better wear performance with higher hardness values can be attributed to the greater resistance of the harder surface against the destructive action of the abrasive particles leading to reduced material loss (Fig. 3, 4). In spite of the presence of the subsurface cracks (Fig. 7c), the hardfaced layer of alloy 2 showed better wear resistance than the substrate (Fig. 3, 4). This implies that these cracks did not affect the wear behavior of the hardfaced layer alloy 2 adversely under the present test conditions. The microcracks can be considerably more effective under severe wear conditions leading to higher wear rates. Improved wear resistance of the harder specimen was further supplemented by the generation of finer debris particles (Fig. 6) and less surface damage (Fig. 5). The smoother abraded surfaces of the harder samples (Fig. 5) were also confirmed with corresponding lower roughness (R_a) values (R_a = 1.2 and 1.28 μm for the hardfaced layers 1 and 2 and 1.48 μm for the substrate) in order of their decreasing hardness property (Table 1).

Increasing wear rate with load (Fig. 3) could be due to a larger depth of indentation made by the abrasive particles (Ref 10). Further, relatively more improvement in the wear characteristics of the hardfaced surfaces over the substrate at larger loads indicates high resistance of the former against the destructive action of the abrasive particles (Ref 10).

The effect of the distance traversed on the wear characteristics of the specimens did not follow a definite trend (Fig. 3). This could be due to several factors including wear-induced subsurface hardening and microcracking tendency during abrasion. Subsurface hardening reduces the wear loss, while microcracking during abrasion produces a reverse effect (Ref 6). The hardfaced layers with high hardness values (Table 1) and hence more brittleness caused less wear-induced subsurface hardening. At the same time, quick removal of the contacting subsurface layer in the case of the harder (hardfaced) layers (through brittle fragmentation) takes place in addition to microcutting (Ref 10). This was also evident from less attachment of regions to the bulk in the subsurface regions of the samples (Fig. 7b, c). Accordingly, the wear rate of the hardfaced layers remained marginally affected with distance (Fig. 3). This could be attributed to a practically counterbalancing effect of the subsurface hardening and the microcracking tendency of the specimens (Ref 6). Increasing wear rate with distance indicates the predominance of the microcracking tendency over subsurface hardening. On the contrary, a reduction in the wear loss with distance suggests the reverse to be effective (Ref 6).

Initial increase in the rate of material loss with distance in the case of the substrate tested at 7 N (Fig. 3) can be attributed to the predominant effect of microcracking tendency. The latter was also observed from the subsurface characteristics of the specimens (Fig. 7a). However, the subsurface hardening became more effective at greater sliding distances causing a reduction in wear rate beyond a specific distance (Fig. 3).

The nature of debris (Fig. 6) and the abraded surfaces (Fig. 5) generated could be explained on the basis of the operating wear mechanisms. Angle of attack of the abrasive particles on specimen surface is an important parameter in this context (Ref 12). For example, machining chips (Fig. 6, regions marked A) are formed by the abrasive particles that attack the specimen surfaces at higher (than the critical) rake angles wherein predominantly microcutting action occurs (Ref 13). Under the circumstances, the abraded surfaces revealed more defined cutting grooves (Fig. 5). On the contrary, microploughing action of the abrading medium takes place as a result of attacking the counteracting surface at subcritical rake angles. This causes the formation of debris in the form of deformed flakes (Ref 13) as shown in Fig. 6(c) in the region marked B.

An appraisal of the observations of this investigation clearly indicates superior wear resistance of the hardfaced layers over that of the substrate. A correlation among the nature of microconstituents, hardness, and the wear response of the specimens also exists. The wear characteristics of the samples were supported by the shape and size of the debris particles and the features of the wear surfaces. The subsurface regions generated in the wear surfaces also supported observations made on wear characteristics of the samples. Regarding the operating material removal mechanisms, microcutting and brittle fragmentation played important roles in the case of the hardfaced layers. Microploughing was also operative in addition to microcutting during abrasion of the substrate. In addition, wear-induced subsurface deformation and a microcracking tendency of the specimens also influenced wear behavior.

5. Conclusions

- Hardfaced layers exhibit better wear resistance (inverse of wear rate) over the substrate; the harder the specimen surface is, the better the (abrasive) wear behavior.
- Wear resistance decreases with load, while distance has a mixed influence.
- Factors controlling wear behavior in this study were observed to be the wear-induced subsurface deformation and microcracking tendency of the specimens.

References

1. C. Allen and B. Ball, A Review of the Performance of Engineering Materials under Prevalent Tribological and Wear Situations in South African Industries, *Tribol. Int.*, Vol 29, 1996, p 105-116
2. O. Scheffler and C. Allen, Abrasive Wear of Steels in South African Soil, *Tribol. Int.*, Vol 21, 1988, p 127-135

3. L. Xu and N. Kennon, A Study of the Abrasive Wear of Carbon Steels, *Wear,* Vol 148, 1991, p 101-112
4. S.J. Quirke, O. Scheffler, and C. Allen, An Evaluation of the Wear Behavior of Metallic Materials Subjected to Soil Abrasion, *Soil and Tillage Research,*Vol 11, 1988, p 27-42
5. R.C.D. Richardson, Wear in Agricultural Machinery: The Relevance of a Study of the Wear of Materials Against Bonded Abrasive, *J. and Proc. Inst. Agric. Eng.*, Vol 19, 1963, p 42
6. B.K. Prasad and S.V. Prasad, Abrasion Induced Microstructural Changes during Low Stress Abrasion of a Plain Carbon (0.5%) Steel, *Wear,* Vol 151, 1991, p 1-12
7. T.H. Shailes, Coating Parts with Hardfacing Alloys: The Cost Effective Solution to Wear, *Prof. Eng.*, Vol 30, 1993, p 56-58
8. Microstructure of Cast Irons, *Atlas of Microstructures of Industrial Alloys,* Vol 7, *Metals Handbook,* 8th ed., American Society for Metals, 1972, p 99
9. P. Crook, Friction and Wear of Hardfacing Alloys, *Friction, Lubrication, and Wear Technology,* Vol 18, *ASM Handbook,* ASM International, 1992, p 758
10. B.K. Prasad, A.K. Jha, O.P. Modi, S. Das, and A.H. Yegneswaran, Abrasive Wear Characteristics of Zn-37.2 Al-2.5 Cu-0.2 Mg Alloy Dispersed with Silicon Carbide Particles, *Mater. Trans., JIM,* Vol 36, 1995, p 1048-1057
11. R. Dasgupta, B.K. Prasad, A.K. Jha, O.P. Modi, S. Das, and A.H. Yegneswaran, Wear Characteristics of a Hardfaced Steel in Slurry, *Wear,* Vol 209, 1997, p 255-262
12. A.T. Alpas and Z. Zhang, Effect of SiC Particulate Reinforcement on the Dry Sliding Wear of Aluminium-Silicon Alloys (A356), *Wear,* Vol 155, 1992, p 83-104
13. S.V. Prasad, P.K. Rohatgi, and T.H. Kosel, Mechanisms of Materials Removal during Low Stress and High Stress Abrasion of Aluminium Alloy-Zircon Particle Composites, *Mater. Sci. Eng.*, Vol 80, 1986, p 213-221